Per. Mineral. (2008), 77, 2, 15-25

doi:10.2451/2008PM0009
http://go.to/permin

PERIODICO di MINERALOGIA
established in 1930

An International Journal of
MINERALOGY, CRYSTALLOGRAPHY, GEOCHEMISTRY, ORE DEPOSITS, PETROLOGY, VOLCANOLOGY
and applied topics on *Environment*, *Archaeometry* and *Cultural Heritage*

Tests of the correlation between composition and morphology of tremolite from Montgomery County, Maryland, USA

MATTHEW S. SANCHEZ [1] and MICKEY E. GUNTER [2,*]

[1] RJ Lee Group Inc., 350 Hochberg Road, Monroeville, Pennsylvania, 15146, USA
[2] Geological Sciences, University of Idaho, Moscow Idaho, 83844, USA

ABSTRACT. — Polished thin sections were prepared of a sample of tremolite from Montgomery County, Maryland and analyzed for major and trace elements of the prismatic and fibrous morphologies. Chemical data were obtained using EPMA (major element), laser ablation ICP-MS (trace element), XRF (whole rock), and the $Fe^{3+}/\Sigma Fe$ ratio was determined by Mössbauer spectroscopy. The polished thin sections were observed with a polarized light microscope (PLM) and photographed to show the textural relationships between the prismatic and fibrous amphiboles. Powder X-ray diffraction (XRD) showed that the sample is a relatively pure tremolite with only traces of clinochlore occurring in the sample. The variation of major elements in the prismatic crystals is less than the variation among the fibrous portion, while the variability in the level of trace elements is greater for the prismatic crystals than the fibrous portion. Multivariate hierarchal cluster analysis was performed in an attempt to correlate composition to morphology. Using the major elements obtained by EPMA, no clustering occurred, while the trace elements obtained from laser ablation ICP-MS, yielded a separation based on morphology.

* Corresponding author, E-mail:mgunter@uidaho.edu

RIASSUNTO. — Sono state preparate sezioni sottili lucide di tremolite proveniente da Montgomery County, Maryland, per la determinazione degli elementi maggiori e in traccia delle morfologie prismatica e fibrosa dell'anfibolo. I dati chimici sono stati ottenuti tramite microsonda elettronica (EMPA) per gli elementi maggiori, microsonda ad ablazione laser (LA-ICP-MS) per gli elementi in traccia e fluorescenza-X (XRF) per l'analisi chimica dell'intera roccia; il rapporto $Fe^{3+}/\Sigma Fe$ è stato determinato tramite spettroscopia Mössbauer. Le sezioni sottili sono state inoltre osservate e fotografate al microscopio a luce polarizzata (PLM), al fine di mostrare le relazioni tessiturali tra gli anfiboli fibrosi e quelli prismatici. La diffrazione a raggi-X su polveri (XRD) ha evidenziato che il campione è composto essenzialmente da tremolite, con tracce di clinocloro. Nei cristalli prismatici la variazione degli elementi maggiori è minore di quella relativa alla porzione fibrosa. Il tentativo di correlare la composizione con la morfologia, tramite analisi gerarchica multivariata, ha evidenziato che gli elementi maggiori, ottenuti in microsonda elettronica, non originano raggruppamenti, mentre per gli elementi in traccia, determinati tramite LA-ICP-MS, si osserva una separazione correlata alla morfologia.

Key words: *tremolite, morphology, composition, asbestiform, nonasbestiform.*

Introduction

Most of the world's asbestos deposits seem to form under very special conditions within rock formations that have undergone deformation. The folding, faulting, shearing, and dilation is commonly accompanied by the intrusion of magma, forming dikes and sills. The mineral fibers crystallize in high strain environments, such as within folds, shear planes, faults, dilation cavities, and at intrusive contacts (Ross and Nolan 2003). Fibers forming in a tensional environment and filling veins are referred to as cross fibers, whereas those forming in a shear environment along active faults are slip fibers.

The major goal of this study was to determine if there existed, and we could determine, differences in the composition of the fibrous and prismatic portions of an amphibole sample in which both morphologies occurred. To accomplish this, we prepared a polished thin section of a hand sample of tremolite in which both morphologies were observed. Then we employed precise compositional determinations of both morphologies and used statistical methods to determine if compositions of the two morphologies were similar or differed. The main reasons to undertake this study were two-fold: 1) to determine if composition controlled morphology and 2) implications that differences in composition might have on the health effects of these materials if inhaled.

Review of the controls on the asbestiform habit

For an extensive review of amphibole asbestos mineralogy, the reader is referred to Zoltai (1981), Ross and Nolan (2003), and Gunter et al. (2007a). These articles highlight many peculiarities of the asbestiform amphiboles over their non-asbestiform varieties. However, the authors do not document any possible chemical controls for the peculiar growth habits of the asbestiform amphiboles.

Statements about major element controls of amphibole morphology are sparse in the literature. Dorling and Zussman (1987) found that the Al content in asbestiform amphiboles of the calcic group do not exceed 0.4-0.6 apfu in the tetrahedral site for the samples they analyzed. Verkouteren and Wylie (2000) concurred that tetrahedral Al content does not exceed 0.5 apfu for fibrous amphiboles samples in the compositional range tremolite-actinolite-ferro-actinolite. Synthetic acicular hastingsite with length > 30 μm and widths < 4 μm are documented to have as high as 2.00 apfu Al content by (Thomas 1982), although this high Al content has not been documented in nature. In recent studies Bandli et al. (2003), Meeker et al. (2003), and Sanchez (2007) found no correlations between major-element composition and morphology in the amphiboles of the Rainy Creek Complex near Libby, Montana. Sanchez (2007) did characterize the levels of trace elements in the fibrous and prismatic amphiboles from Libby and found some weak correlations between composition and morphology. Gianfagna and Oberti (2001) and Gianfagna et al. (2007) characterized prismatic and fibrous fluoro-edenite using micro-chemical, Mössbauer, and structural refinement. They determined that Fe^{2+} is preferentially located at the M2 site, whereas Fe^{3+} was found exclusively at the M3 site for this fibrous amphibole. They also determined that the $Fe^{3+}/\Sigma Fe$ ratio, as obtained by Mössbauer spectroscopy, is less for the fibrous morphology.

The possible role of trace elements to the crystal habit or crystal growth of asbestiform and non-asbestiform amphiboles has not been studied to our knowledge. However, research has been ongoing on the incorporation of trace elements in other mineral groups and possible correlations with crystal habit. In a recent study using *in situ* AFM, Wasylenki et al. (2005) explored the growth of calcite in saturated Sr solutions. The addition of Sr to the calcite growth system leads to significant changes in growth hillock morphology. Hillocks became elongate perpendicular to the projection of the *c*-glide plane. An earlier study by Northrup and Reeder (1994) on trace-element distribution in topaz using differential interference contrast microscopy showed that the dominant (110) form exhibits large, polygonized, spiral-growth hillocks with four faces, each comprising an array of parallel growth-steps. The authors stated that "there is precise correlation between surface

microtopography and trace-element distribution, demonstrating a surface-structural control of trace element incorporation."

Sample preparation and analysis

The tremolite used in this study was collected in Montgomery County, Maryland, in a serpentinite from an ophiolite sequence (Ross and Nolan 2003). Chrysotile also occurs in this sequence. Fig. 1a is a photograph of the bulk sample; it is approximately 20 cm in length. Both the EPMA and laser-ablation ICP-MS analyses were performed on the same thin section, whereas photographs of the structural features were taken on another. In preparation for EPMA, the thin section was observed using a polarizing light microscope (PLM) and seven areas of interest were marked that contained intergrown prismatic and fibrous grains. Fig. 1b and 1c show the polished thin section in plane polarized (B) and cross-polarized (C) light with a field of view of 4.5 cm. The seven marked areas can be seen, and the other markings are used for slide orientation purposes while using the microprobe.

Powder X-ray diffraction (XRD) was used to determine if any other mineral phases are present in the sample. Four grams of the sample was ground using a mortar and pestle. The sample was back-filled into a XRD mount and analyzed using a Siemens D-5000 diffractometer located at the University of Idaho. We used Cu Kα radiation at 40 kv and 30 mA. The scan range started at 2° 2-theta and ended at 40° 2-theta with step increments of 0.02° and count times of 9 seconds per step. Mineral phases were identified using the software program EVA. No quantitative analysis was attempted owing to the small amount of the clinochlore phase.

X-ray fluorescence (XRF) was used to determine the bulk chemistry of the sample. Two XRF beads were prepared by taking 20 g of sample, wet grinding, sieving the ground amphibole, and using the <200 mesh size fraction. Next, glass beads were made using a 3.5 g of sample, and mixing that with 7.5 g of Li tetraborate and heating to 1000 °C. The two glass beads were analyzed at the GeoAnalytical Laboratory at Washington State University using a Rigaku 3370 XRF. This was the same sample used in Gunter et al. (2007b) as an

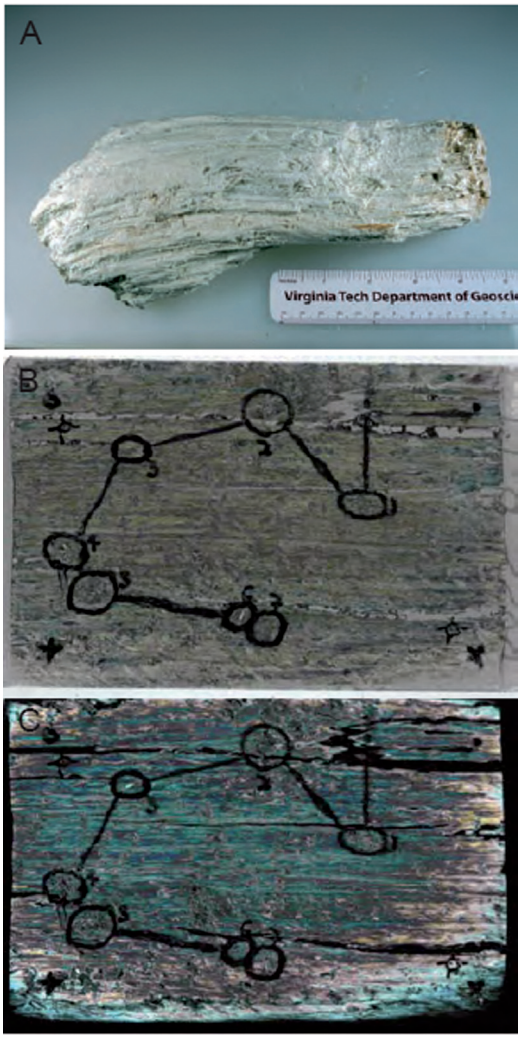

Fig. 1 – Photographs illustrating sample preparation. (A) The hand sample of tremolite from Montgomery County, Maryland; which predominantly consists of fibrous tremolite. (B) Polished thin section in plane-polarized light with areas of interest marked out for EPMA. (C) The same polished thin section in cross-polarized light with seven areas of interest marked out for EPMA. For 1B and 1C, the field of view is 4.5 cm.

SEM-EDS (scanning electron microscope – energy dispersive analysis) standard for compositional analysis of amphiboles.

Electron-probe microanalysis (EPMA) was used to characterize the major- and minor-element

composition, in terms of Si, Al, Ti, Fe, Mn, Mg, Ca, K, Na, Cl, and F. The wavelength-dispersive analyses were carried out using a Cameca Camebax electron microprobe at the Washington State GeoAnalytical Laboratory. We used an accelerating voltage of 15 kV, beam current of 12 nA, and a beam diameter of 2 μm. The appropriate ZAF corrections were performed. The following standards were used: Si and Al (Wilberforce hornblende), Ti (titianite), Fe (Rockport fayalite), Mn (spessartine), Mg (forsterite), Ca (diopside), K (orthoclase), Na (albite), Cl (sylvite), and F (phlogopite). Total Fe was measured as FeO, and the appropriate proportions of Fe^{2+} and Fe^{3+} using the $Fe^{3+}/\Sigma Fe$ ratio determined by Mössbauer spectroscopy at Mt. Holyoke College. The amphibole species was determined using the IMA classification as outlined in Leake et al. (1997) as tremolite.

Laser-ablation ICP-MS at the Washington State University GeoAnalytical laboratory was used to determine the levels of trace elements composition in the same areas analyzed by EPMA. The spectrometer is an Element2 with a New Wave UP213 Nd-YAG laser, which was operated at 20 Hz and delivered 10-15 J/cm^2 to the polished samples surface; the carrier gas was helium. Calibration was done using the following two standards, BCR-2G and NIST 610. A total of 31 elements were analyzed and corrected for background. Data for the 31 elements were normalized to Si as determined by EPMA. The laser-burned trenches were approximately 8 μm in width and did not penetrate through the sample.

Results and Discussion

Formation of this fibrous amphibole took place in a shear environment. Fig. 2 is a series of photographs showing textures apparent within the thin sections. The tremolite sample shows a range

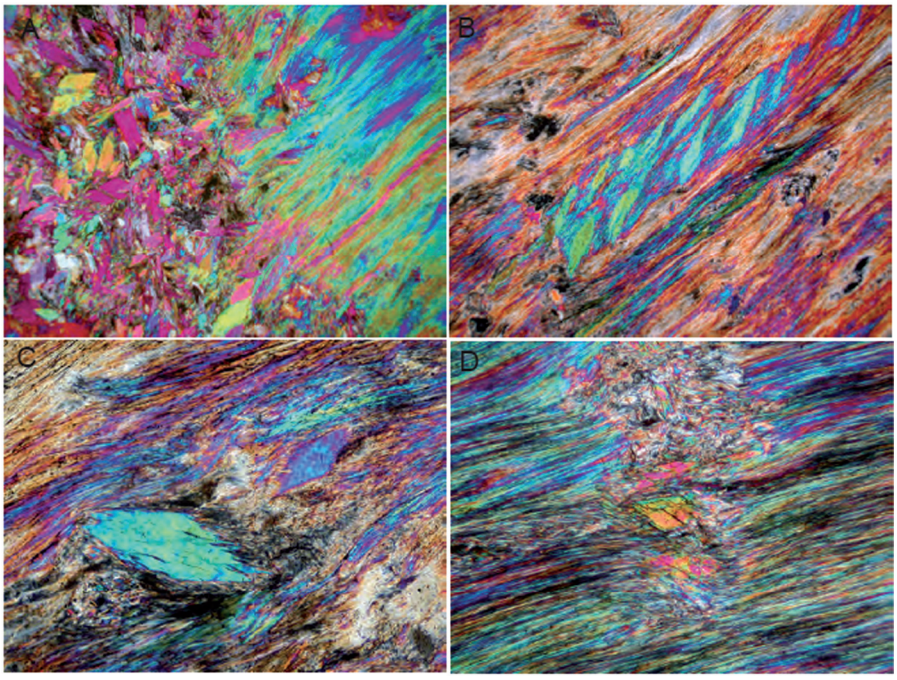

Fig. 2 – A series of PLM images in cross-polarized light with full-wave plate inserted. Crystals are oriented so that maximum brightness is shown. (A) Contact between prismatic crystals of tremolite and fibrous morphology. (B) A series of prismatic tremolite *en echelon* caused by shear. (C) and (D) Prismatic grains in contact with fibrous grains creating sigma grain structures. Field of view for each photograph is 2 mm.

of crystal morphologies. In Fig. 2a, we illustrate an interface between prismatic crystals grading into fibrous amphiboles. In Fig. 2b, we show five prismatic *en echelon* crystals reflecting growth in a shear-stress environment, also the grains shown in Fig. 2c and 2d grew in shear stress environments. Grain boundaries are distinct but not sharp, and the prismatic and fibrous crystals are pre- to synkinematic with respect to the deformation. The formation of this tremolite is consistent with the geological conditions for slip-fiber growth and common criteria for the formation of asbestiform minerals (i.e., part of an intensely deformed ophiolite sequence).

The powder diffraction scan (Fig. 3) reveals only one other mineral phase is present in detectable amounts: clinochlore. The identification of this phase was done using the computer software EVA and substantiated using the chemical data obtained by XRF and EPMA (Table 1). The XRF-derived composition would contain influence from the clinochlore phase, (i.e. higher concentrations of Si, Al, Mg and Fe). Only the elements with significant concentrations are reported. The XRF results have greater concentrations of Si, Al, Fe, and Na, but Mg is similar to that of the EPMA data. The chlorite is therefore an Fe rich phase. The variability of Si, Al, Fe and Mg is greater in the fibrous samples than in the prismatic crystals analyzed by EPMA, possibly owing to the absence of the chlorite in the prismatic crystals, or because the fibrous samples have a poorer polish. The variances of the other elements are almost identical between the prismatic and fibrous amphiboles. Concerns due to the greater chemical variability in the fibrous grains will be discussed later.

Morphological distinctions between prismatic and fibrous amphiboles were determined based on the following criteria. Prismatic amphiboles show distinct euhedral faces, in many cases {110}. The fibrous amphibole do not show distinct faces at PLM resolution and occur as intergrown masses of fibers. Fig. 4 illustrates the differing morphologies. Fig. 4a and 4b are photographs of a prismatic crystal taken through the optical system of the electron microprobe in reflected and transmitted light; the field of view is 200 μm. Fig. 4c and 4d are photographs of a fibrous example taken in the same manner. Each analyzed point was photographed, and the morphology was determined. The reflected-light (C) photograph shows that even the fibrous amphibole had a good polish for analysis; thus removing the possibility of the two forms having differing qualities of

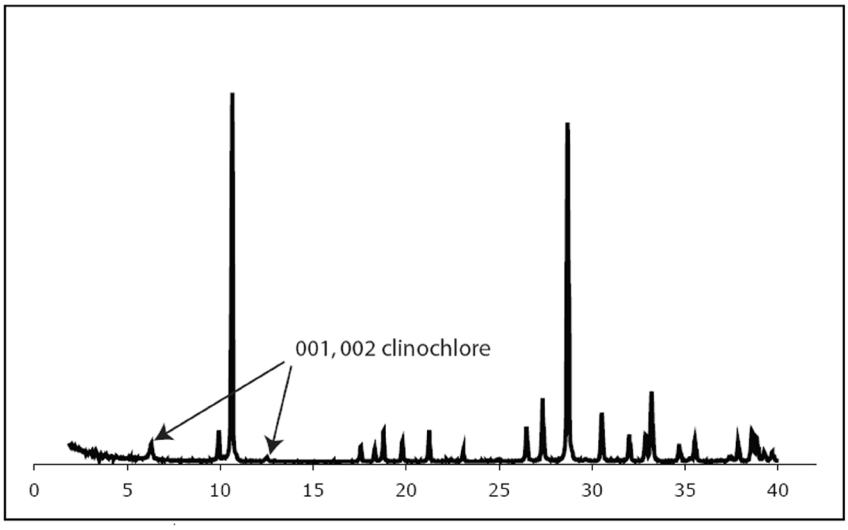

Fig. 3 – Powder X-ray diffraction pattern for the Montgomery, Maryland tremolite. Mineral phases present in the sample is predominantly tremolite with minor amounts of clinochlore. The 001 and 002 reflections are identified. The X-ray diffraction data confirm XRF and EPMA data that this tremolite sample is relatively pure.

Table 1 — *Compositional data obtained from different methods for the tremolite sample used in this study. The EPMA analysis is segregated into prismatic and fibrous. Wt% oxide, number of analyses, apfu, and Mg # values are given*

Wt%	XRF	EPMA Prismatic	EPMA Fibrous
SiO_2	58.87	57.25 (0.83)	57.12 (1.03)
Al_2O_3	0.43	0.06 (0.05)	0.15 (0.21)
$FeO_{Measued}$	4.13	3.46 (0.70)	4.06 (0.79)
MnO	0.02	0.13 (0.03)	0.11 (0.04)
MgO	22.45	22.55 (0.48)	22.09 (0.70)
CaO	13.66	13.21 (0.17)	13.21 (0.28)
Na_2O	0.11	0.02 (0.02)	0.02 (0.01)
H_2O	-	2.13 (0.04)	2.12 (0.04)
F	-	0.06 (0.05)	0.07 (0.05)
$Fe^{3+}/\Sigma Fe$	0.19	0.19	0.19
Fe_2O_3	0.87	0.73	0.87
FeO	3.35	2.80	3.27
Total	99.76	98.95 (1.01)	99.05 (1.48)
n	-	55	61
apfu			
Si	8.10	7.95	7.94
Al	0.05	0.01	0.02
Fe^{3+}	0.09	0.08	0.09
Fe^{2+}	0.38	0.35	0.38
Mn	0.00	0.01	0.01
Mg	4.63	4.66	4.58
Ca	1.99	1.96	1.96
Na	0.03	0.01	0.01
H	2.00	1.97	1.97
F	-	0.03	0.03
$Mg/(Fe^{2+}+Mg)$	0.92	0.93	0.92

surface. Figs. 4e (plane-polarized) and 4f (cross-polarized with full wave plate inserted) show the areas that were analyzed using laser ablation ICP-MS in circle 5 (Cr5) as seen through the PLM

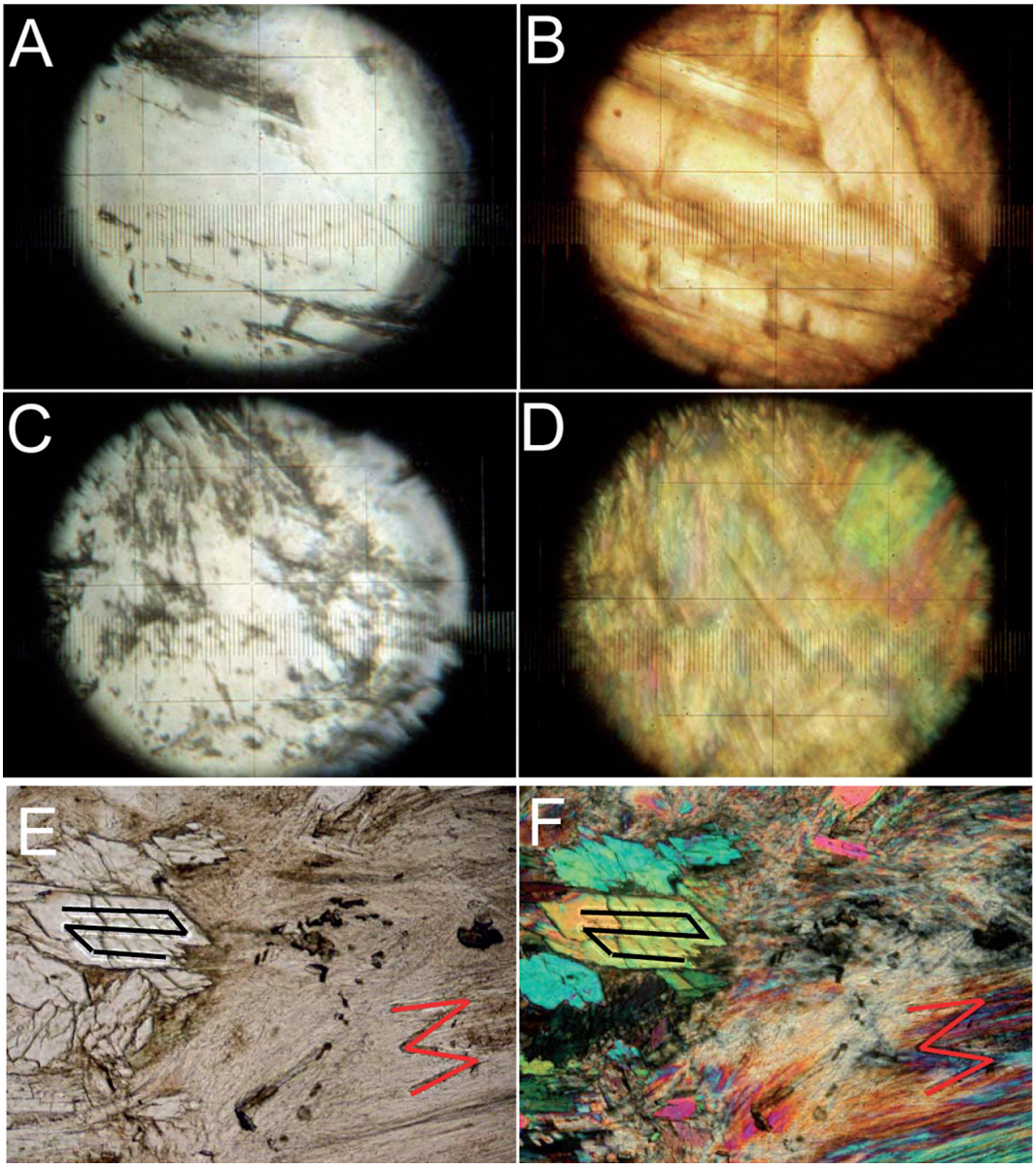

Fig. 4 – Photographs illustrating what was determined as fragment and fibers for both EPMA and LA-ICP-MS analyses. (A) and (B) An example of a fragment as seen through the electron microprobe optical system in reflected and transmitted light. Field of view is 200 μm. (C) and (D) Examples of a fiber as seen through the optical system of the electron microprobe in transmitted and reflected light. Field of view is 200 μm. (E) and (F) Photographs taken with a PLM showing the areas that were analyzed using LA-ICP-MS. The field of view is 1.2 mm. The black marked laser-burned trench is a fragment and the red marked laser-burned trench is a fiber.

post analysis; the field of view is 1.2 mm. The laser-burned trench traced in black is an example of prismatic morphology, whereas the laser-burned trench traced in red is an example of fibrous morphology.

In Table 2a, we present the trace-element data for the six prismatic crystals analyzed by laser

Table 2a — *Trace-element data (in ppm) obtained with LA-ICP-MS for six prismatic tremolite crystals. (Cr# refers to circle number in which the analysis was obtained)*

	Cr2_pris	Cr3_pris	Cr4_pris	Cr5_pris	Cr6_pris	Cr6_pris2
Ca43	8.79	9.77	7.74	7.63	7.96	7.88
Sc45	5.63	-1.14	3.16	3.35	2.83	8.09
Ti47	40.33	180.25	35.83	59.32	62.34	40.74
Rb85	0.01	0.01	-0.01	0.01	0.00	0.35
Sr88	3.28	4.27	3.32	3.35	2.79	5.24
Y89	0.87	5.24	0.75	1.34	2.58	1.20
Zr90	0.10	0.37	0.19	0.22	0.43	0.69
Nb93	0.00	0.00	0.00	0.00	0.00	-0.01
Cs133	0.00	0.00	0.01	0.00	0.00	0.03
Ba138	0.08	0.05	0.01	0.16	0.07	2.05
La139	0.03	0.06	0.03	0.03	0.03	0.08
Ce140	0.07	0.26	0.08	0.08	0.14	0.11
Pr141	0.02	0.10	0.01	0.02	0.04	0.04
Nd146	0.14	0.83	0.15	0.25	0.30	0.26
Sm147	0.07	0.31	0.03	0.06	0.19	0.16
Eu151	0.01	0.17	0.02	0.02	0.09	0.02
Gd157	0.11	0.37	0.05	0.11	0.21	0.17
Tb159	0.02	0.09	0.02	0.03	0.05	0.03
Dy163	0.15	0.59	0.14	0.22	0.34	0.19
Ho165	0.03	0.12	0.02	0.04	0.07	0.03
Er166	0.06	0.39	0.02	0.10	0.21	0.09
Tm169	0.01	0.08	0.01	0.01	0.03	0.00
Yb172	0.04	0.53	-0.01	0.07	0.28	0.04
Lu175	0.01	0.05	0.00	0.01	0.02	0.00
Hf178	0.02	0.02	0.00	-0.01	0.00	0.03
Ta181	-0.02	-0.01	-0.01	-0.02	0.00	-0.01
Pb206	0.04	0.07	0.08	0.06	0.14	0.24
Pb207	0.15	0.11	0.14	0.09	0.05	0.13
Pb208	0.06	0.10	0.10	0.08	0.06	0.08
Th232	-0.01	0.00	0.00	0.00	0.00	0.00
U238	0.00	0.00	0.00	0.00	0.00	0.00

TABLE 2B — *Trace-element data (in ppm) obtained with LA-ICP-MS for six fibrous tremolite areas in the thin section. (Cr# refers to circle number in which the analysis was obtained)*

	Cr2_fiber	Cr3_fiber	Cr4_fiber	Cr5_fiber	Cr6_fiber	Cr6_fiber2
Ca43	8.01	8.77	6.75	7.11	7.76	7.5
Sc45	2.58	2.46	3.08	3.22	4.59	2.63
Ti47	80.72	106.81	81.13	60.90	77.96	70.27
Rb85	0.07	0.07	0.15	0.08	0.21	0.20
Sr88	2.82	3.34	2.50	2.48	2.77	2.40
Y89	1.85	2.87	1.73	1.07	1.88	1.49
Zr90	0.52	0.78	0.81	0.75	1.05	0.74
Nb93	0.01	0.02	0.01	0.01	0.00	0.01
Cs133	0.01	0.01	0.02	0.02	0.01	0.00
Ba138	0.25	0.34	0.61	0.83	0.46	0.42
La139	0.04	0.05	0.05	0.05	0.02	0.03
Ce140	0.08	0.11	0.10	0.06	0.09	0.07
Pr141	0.03	0.04	0.03	0.02	0.03	0.02
Nd146	0.20	0.33	0.21	0.15	0.25	0.17
Sm147	0.14	0.18	0.12	0.05	0.13	0.10
Eu151	0.04	0.09	0.05	0.02	0.05	0.03
Gd157	0.14	0.20	0.15	0.10	0.15	0.09
Tb159	0.04	0.06	0.04	0.02	0.03	0.03
Dy163	0.27	0.39	0.27	0.16	0.30	0.19
Ho165	0.05	0.08	0.05	0.04	0.08	0.04
Er166	0.16	0.25	0.17	0.09	0.23	0.12
Tm169	0.03	0.04	0.03	0.02	0.03	0.03
Yb172	0.14	0.28	0.20	0.09	0.20	0.17
Lu175	0.02	0.05	0.03	0.02	0.03	0.03
Hf178	0.02	0.02	0.03	0.03	0.01	0.02
Ta181	0.00	0.00	0.00	0.00	0.00	0.00
Pb206	0.02	0.04	0.40	0.12	0.18	0.14
Pb207	0.07	0.64	0.36	0.12	0.18	0.17
Pb208	0.06	0.09	0.31	0.12	0.16	0.15
Th232	0.00	0.00	0.01	0.00	0.00	0.00
U238	0.00	0.00	0.00	0.00	0.00	0.00

ablation ICP-MS. Table 2b contains the analogous data for the six fibrous sample areas analyzed. Interestingly, the variability of the trace elements in the prismatic crystals was greater than their variability in the fibrous amphiboles. This is opposite to the variability noted in the EPMA data.

Cluster analysis was chosen as the statistical method most suitable for our data. It was chosen over determinant analysis because no assumptions of morphology are needed. The morphological habits of the tremolite are known, but we were interested in a possible control on the morphology. Using the statistical computer software JMP by SAS (Statistical Analysis Software), Ward's hierarchical cluster was chosen due to the small dataset being used.

Using the major elements obtained using EPMA, the clusters produced did not distinguish between the prismatic and fibrous amphiboles. However, using only the trace-element data obtained by laser-ablation ICP-MS, the prismatic and fibrous amphiboles clustered, the one outlier being a prismatic crystal. The Ti content of this sample is large when compared to the other samples. The results of the cluster analysis for the trace elements are shown in Fig. 5; marked in red are those samples determined as fibrous and in black are the prismatic samples. Using this limited number of samples, the fibrous tremolite clustered. However, this correlation between morphology and trace element content is tentative at best. The presence of trace amounts of clinochlore intergrown with the fibrous tremolite could potentially influence the clustering, because as mentioned above, the variation of the trace elements in the prismatic crystals is greater than that of the fibers.

There does appear to be grounds for a more detailed study into the role of trace elements on amphibole morphology. A deeper understanding of the role of trace elements in crystal growth and habit would help the medical community concerned with the pathology of asbestos-related disease to acquire a better understanding of the biological processes occurring in the lungs when these materials are inhaled.

Acknowledgements

We would like to thank Malcom Ross for the tremolite sample used in this study, Scott B. Cornelius and Charles Knaack of the Washington State GeoAnalytical Laboratory for their assistance in data collection, and M. Darby Dyar of Mt. Holyoke College for Mössbauer analysis. Also, we would

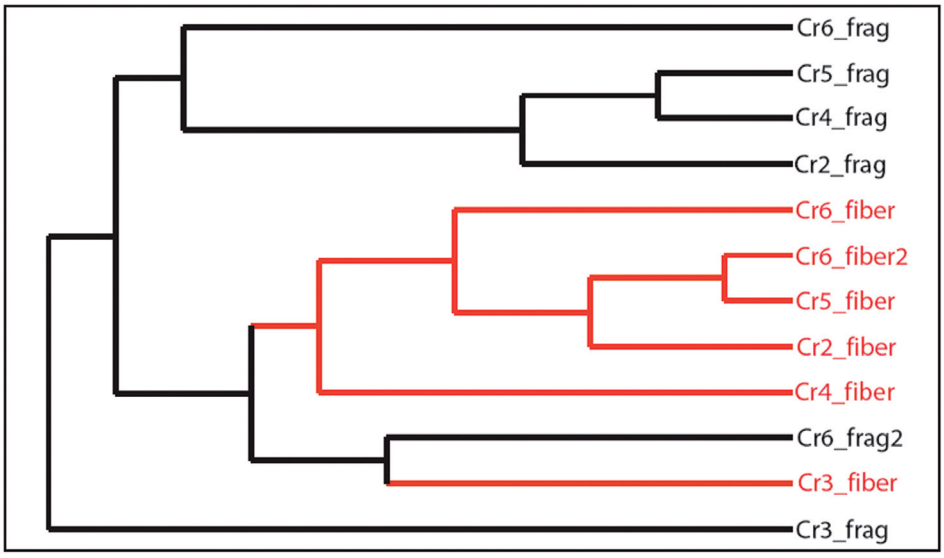

Fig. 5 – Cluster analysis for trace elemental data, the fibrous morphologies are in red while the prismatic morphology is in black. The fibrous tremolite clustered. The only outlier is a prismatic crystal.

like to thank Bob Martin and John Addison for their helpful comments.

REFERENCES

Bandli B.R., Gunter M.E., Twamley B., Foit F.F., Jr. and Cornelius S.B. (2003) - *Optical, compositional, morphological, and X-ray data on eleven particles of amphibole from Libby, Montana, U.S.A.* Can. Mineral., **41**, 1241-1253.

Dorling M. and Zussman J. (1987) - *Characteristics of asbestiform and non-asbestiform calcic amphiboles.* Lithos, **20**, 469-489.

Gianfagna A. and Oberti R. (2001) - *Fluoro-edenite from Biancavilla (Catania, Sicily, Italy): Crystal chemistry of a new amphibole end-member*. Am. Mineral., **86**, 1489-1493.

Gianfagna A., Andreozzi G.B., Ballirano P., Mazziotti-Tagliani S. and Bruni B.M. (2007) - *Structural and chemical contrasts between prismatic and fibrous fluoro-edenite from Biancavilla, Sicily, Italy.* Can. Mineral., **45**, 249-262.

Gunter M.E., Belluso E. and Mottana A. (2007a) - *Amphiboles: environmental and health concerns.* In Amphiboles: Crystal Chemistry, Occurrences, and Health Concerns. Rev. Min. Geoch., **67**, 453-516.

Gunter M.E., Sanchez M.S. and Williams T.J. (2007b) - *Characterization of chrysotile samples for the presence of amphiboles, Carey Canadian Deposit, Southeastern Quebec, Canada.* Can. Mineral., **45**, 263-280.

Leake B.E., Woolley A.R., Arps C.E.S., Birch W.D., Gilbert M.C., Grice J.D., Hawthorne F.C., Kato A., Kisch H.J., Krivovichev V.G., Linthout K., Laird J., Mandarino J.A., Maresch W.V., Nickel E.H., Rock N.M.S., Schumacher J.C., Smith D.C., Stephenson N.C.N., Ungaretti L., Whittaker E.J.W. and Youzhi G. (1997) - *Nomenclature of the amphiboles: Report of the subcommittee on amphiboles of the International Mineralogical Association, Commission of New Minerals and Mineral Names.* Am. Mineral., **82**, 1019-1037.

Meeker G.P., Bern A.M., Brownfield I.K., Lowers H.A., Sutley S.J., Hoefen T.M. and Vance J.S. (2003) - *The Composition and Morphology of Amphiboles from the Rainy Creek Complex, near Libby, Montana*. Am. Mineral., **88**, 1955-1969.

Northrup P.A. and Reeder R.J. (1994) - *Evidence for the importance of growth-surface structure to trace element incorporation in topaz.* Am. Mineral., **79**, 1167-1175.

Ross M. and Nolan R.P. (2003) - *History of asbestos discovery and use and asbestos-related disease in context with the occurrence of asbestos within ophiolite complexes.* Geol. Soc. Am., Special paper **373**, 448-471.

Sanchez M.S. (2007) - *Characterization of Amphiboles from Libby, Montana.* M.S. Thesis, University of Idaho, Moscow, Idaho, U.S.A.

Thomas M.T. (1982) - *Stability relations of the amphibole hastingsite.* Am. J. Sci., **282**, 136-164.

Verkouteren J.R. and Wylie A.G. (2000) - *The tremolite-actinolite-ferro–actinolite series: Systematic relationships among cell parameters, composition, optical properties, and habit, and evidence of discontinuities.* Am. Mineral., **85**, 1239-1254.

Wasylenki L.E., Dove P.M., Wilson D.S. and De Yoreo J.J. (2005) - *Nanoscale effects of strontium on calcite growth: An in situ AFM study in the absence of vital effects.* Geoch. Cosm. Acta, **69**, No. 12, 3017–3027.

Zoltai T. (1981) - *Amphibole Asbestos Mineralogy.* Reviews in Mineralogy, Volume **9A**, Amphiboles and Other Hydrous Pyriboles-Mineralogy, 237-278.Zoltai,T. (1981) - *Amphibole Asbestos Mineralogy.* Reviews in Mineralogy, Volume 9A, Amphiboles and Other Hydrous Pyriboles-Mineralogy, 237-278.